

## **Simplified Analytical Model for Across-Wind Response of Chimneys Around Critical Wind Velocity Regions**

N. Lakshmanan<sup>1</sup>, G. Ramesh Babu<sup>2</sup>, Devdas Menon<sup>3</sup> and S. Arunachalam<sup>4</sup>

<sup>1</sup>Formerly Director, CSIR-SERC, Chennai, India, [nlaxman@gmail.com](mailto:nlaxman@gmail.com)

<sup>2</sup>Principal Scientist, CSIR-SERC, Chennai, India, [gramesh@serc.res.in](mailto:gramesh@serc.res.in)

<sup>3</sup>Professor, Department of Civil Engineering, IIT Madras, Chennai, [dmenon@iitm.ac.in](mailto:dmenon@iitm.ac.in)

<sup>4</sup>Formerly Chief Scientist, CSIR-SERC, Chennai, India, [sarunacha@yahoo.co.in](mailto:sarunacha@yahoo.co.in)

### **Introduction**

There is an exponential growth in infrastructural facilities in countries like India. Power plant structures constitute a major portion of these structures. Over the last decade, a number of problems of tall chimneys of height ranging from 225 m to 280 m have been studied by CSIR-Structural Engineering Research Centre, a National laboratory under the Council of Scientific and Industrial Research, Government of India. Wind tunnel studies on aero-elastic models of chimneys under simulated atmospheric boundary layer conditions with and without rigid models of interfering power plant structures have been carried out. A number of chimneys were also proof checked for their design carried out by a number of industrial houses. The discussions with the designers have clearly revealed that they are most uncomfortable when they use code recommendations which are extremely complex to comprehend. Researchers and academicians would like to have the designer recommendations in line with the state of the art knowledge on the topic. One such area where possibly simplification to code recommendations would be extremely helpful is the evaluation of across wind response tall chimneys having circular cross section.

A fixed circular cylinder in the path of a uniform oncoming flow forces it to separate and form two shear layers with building up of vortices. The vortices increase in strength, then gets separated forming a periodic vortex street down stream of the cylinder. The problem becomes more complex when there is turbulence in the incident flow. The problem is more complicated when the cylinder has flexibility which introduces fluid-structure interaction. When the oscillations of the cylinder become significant, the dynamics of the flow and the structure become dependant on the motion of the body itself. It is no wonder then that the resulting motion is extremely non-linear. Wind tunnel testing on properly scaled models in simulated boundary layer flows is expected to provide the best estimates of dynamic response. However the inability to achieve equality of Reynolds number in the wind tunnel tests with those existing in full scale conditions had prompted Vickery (1984) to “doubt whether or not this is the best techniques for structures with circular cross sections”. He however suggested that in the case of more complex aerodynamic situations such as those associated with grouped chimneys, wind tunnel studies are better employed to explore the general behaviour for gaining better understanding. However Tamura (1990) observed that wind tunnel tests could be relied upon to predict the behaviour of the reinforced concrete chimneys”. He validated his observation by comparison of full scale tip acceleration of a RC chimney with those predicted from wind tunnel tests.

Holmes (2001) compared the estimated maximum rms tip deflections of three structures with circular cross section using three different codal approaches and concluded clearly, the significant variations exist in estimated response. It is not as if the variations were either uniform over-estimation or under-estimation. Devdas Menon and Srinivasa Rao(1997) studied the uncertainties involved in codal recommendations for across wind load analysis of reinforced concrete

chimneys. They concluded the probability distribution of across wind base bending moment based on Monte Carlo simulation indicates that the overall uncertainty in the estimated moment is very high, the coefficient of variation being as high as 0.50. This is not totally unexpected with the number of parameters that affect across wind response, and the approximations made in analytical modeling at various stages. Very recently Flaga and Lipecki(2010) compared the maximum tip displacement due to vortex excitation on six RC chimneys and showed large scatter as shown in Fig. 1 and the variation being not one directional.

Under such circumstances, there is enough justification to attempt at a much simpler model based on wind tunnel tests, and one of the widely accepted code recommendations. The ACI code recommendations (2008) are based on the extensive work carried out by Vickery and coworkers (1983, 1984, 1995). The developed model is phenomenological in nature and under the fundamental mode; the rms amplitude is given by

$$\tilde{\sigma}_{ac} = \frac{1}{K_{eq}} \left[ \frac{\pi f_0}{4 \xi_T} \cdot S_{Fc} \right]^{1/2} \tag{1}$$

where  $k_{eq}$  = generalized stiffness,

$f_0$  = fundamental frequency

$\xi_T$  = total damping

and  $S_{Fc}$  = Spectral ordinate of the generalized lift force at  $f_0$

The total damping includes structural damping and a negative aerodynamic damping which is dependant on a number of parameters including the height of the chimney, the equivalent diameter, and the thickness of the chimney, intensity of turbulence and the ratio of  $\bar{V}/V_{cr}$ . The derivation of the generalized lift force has involved modified intensity of turbulence and its relation with the lift force coefficient  $\tilde{C}_L$ , effect of aspect ratio  $h/d(u)$  on  $\tilde{C}_L$ , the correlation of fluctuating lift forces due to vortex shedding at two levels  $z_1$  and  $z_2$ , a narrow banded lift force spectrum with a band width parameter dependant on intensity of turbulence, and the fundamental mode shape. If one were to go back to along wind resonant response, the rms amplitude is given by

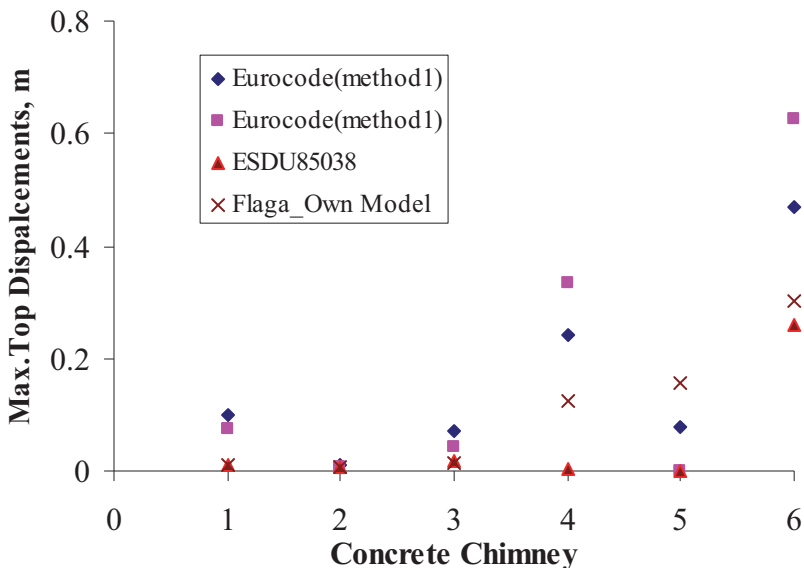


Fig. 1. Comparison of across-wind tip deflection (Flaga-2010).

$$\tilde{\sigma}_{al} = \frac{1}{K_{eq}} \cdot \chi(f_0) \left[ \frac{\pi f_0}{4\xi} S_{F_{al}} \right]^{1/2} \quad (2)$$

Where  $\chi(f_0)$  = aerodynamic admittance value at  $f_0$

$$\frac{\pi f_0}{4\xi} = \int_0^{\infty} \left[ \frac{1}{(1-\eta^2)^2 + 4\xi^2 \eta^2} \right] d\eta \quad (3)$$

Frequency ratio,  $\eta = f / f_0$ , and  $\xi$  = damping factor

Considering that the rms amplitudes are dependant on square root of damping factor, which itself can vary over a wide range, omission of negative aero-dynamic damping may lead to an error of less than 10% in overall estimation particularly in reinforced concrete chimneys in across wind response. Comparing equations (1) and (2), one may generally conclude that all the efforts that have gone in developing the rms amplitude of across wind response is to evaluate a pseudo aerodynamic admittance function including the effects of all known variables. Can this process be made simple? This paper tries to find an answer to this interesting question.

### Wind Tunnel Tests on Models of Chimneys

The typical dimensions and other details of the chimneys tested are given in Table 1. The models are made of aircraft grade aluminum, the mass density of which is nearly the same as that of reinforced concrete. However, the modulus of elasticity of aluminum is nearly twice that of reinforced concrete which would lead to 40 to 50% increase in natural frequency. It was felt that keeping the velocity ratio as 1:1 would be beneficial.

This was achieved by mounting the model chimneys on a circular flexible plate fixed rigidly to the turn table as shown in Fig. 2. The models were tested under simulated open terrain conditions to model scale ratios of 1 in 250 to 1:300. The variation of wind characteristics were measured using a traversing mechanism, and CTA anemometry. The power law exponent for mean velocity profile is 0.165. All the chimneys were instrumented by strain gauges for along wind and across wind bending moments at the base. Full bridge strain gauge instrumentation was adopted, and the sensitivities of in terms of N-m/V were directly obtained using suitable calibration techniques. Also the accelerations at top of the models of chimneys in the along wind and across wind directions were measured. Global lab software was used for data acquisition and analysis of time history records of the measured quantities. The mean wind speed at top of chimneys was

Table 1. Dimensions of the models of chimneys chosen for the study.

S.No	Height of chimney, mm	Bottom outer dia, mm	Top outer dia, mm	Thickness at bottom, mm	Thickness at top, mm	Natural frequency, Hz	Remarks
Chm1	880	83.11	20.12	3.34	1.0	115	Uniform tapered, 1:250 scale
Chm2	720	75.45	23.72	2.79	1.00	158	Uniform tapered, 1:250 scale
Chm3	900	96.33	69.33	3.0	1.33	93	Tapered up to 533.33mm + straight for remaining portion, 1:300 scale
Chm4	900	93.0	53.33	2.66	1.167	100	1/27 Taper up to 533.33mm + almost straight for remaining portion, 1:300 scale
Chm5	1080	135	76	3.47	1.60	73	Tapered up to 820 mm + straight for remaining portion, 1:250 scale

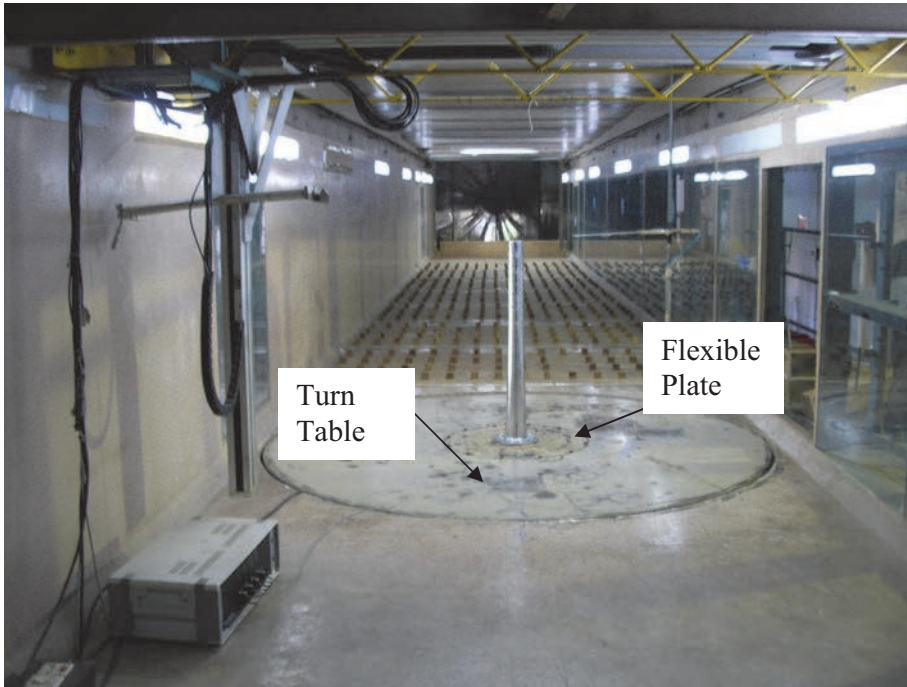


Fig. 2. View of a Typical Chimney Model tested in the Wind Tunnel.

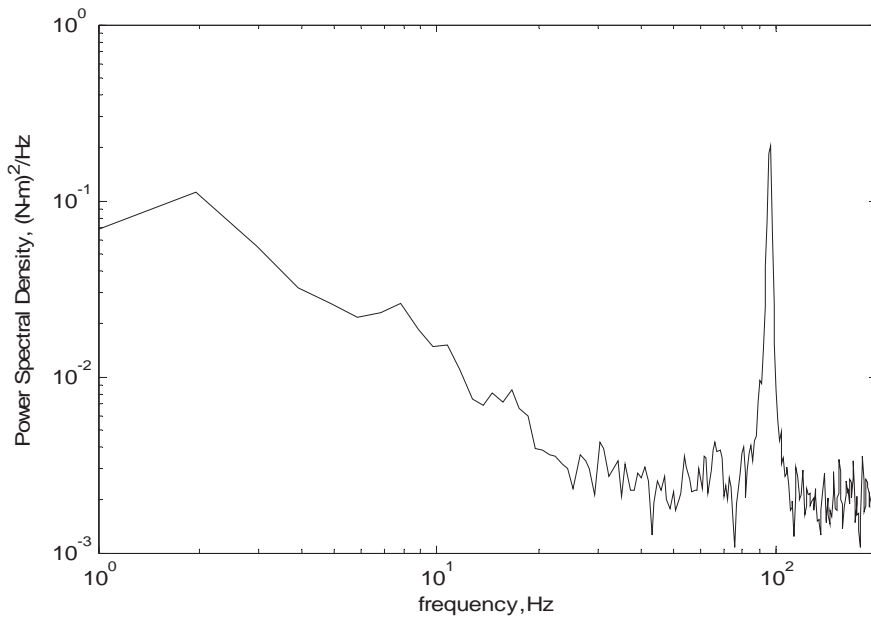


Fig. 3. Spectrum of along-wind base bending moment ( $V = 18.9$  m/s) – Chm4.

incremented in suitable steps. The time history record of acceleration was double integrated numerically to obtain fluctuating deflection time histories. The spectra of along-wind and across-wind bending moments as well as displacements were obtained using custom tailored programs in MATLAB software. Typical spectra obtained in models of chimneys are shown in Figs. 3 to 6.

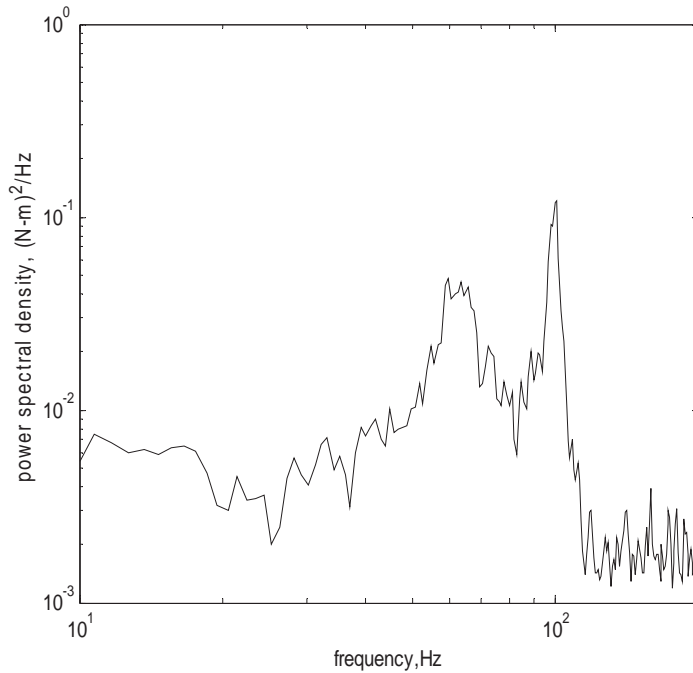


Fig. 4. Spectrum of across base bending moment ( $V = 18.9$  m/s) – Chm4.

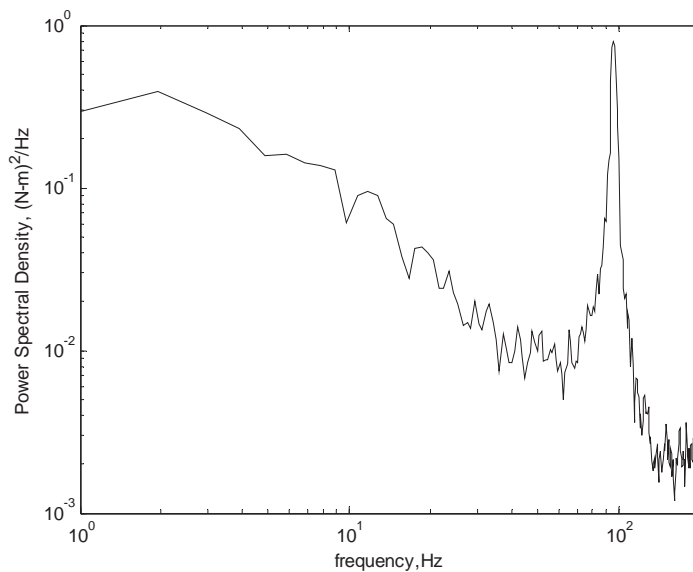


Fig. 5. Spectrum of the along wind base Bending moment ( $V = 28.65$  m/s) – Chm4.

The variance of along wind resonant components was obtained by integrating the spectra around the resonant region. The spectra of across wind bending moment show the response in the vortex shedding region as also the resonant region. As the wind speed is increased the vortex shedding region enters the resonant region leading to large increase in responses. From the figures of across wind responses it was also be seen that when the chimneys have uniform diameter for the top 1/3<sup>rd</sup> region of the chimney, the vortex shedding region has a lower band width, as compared

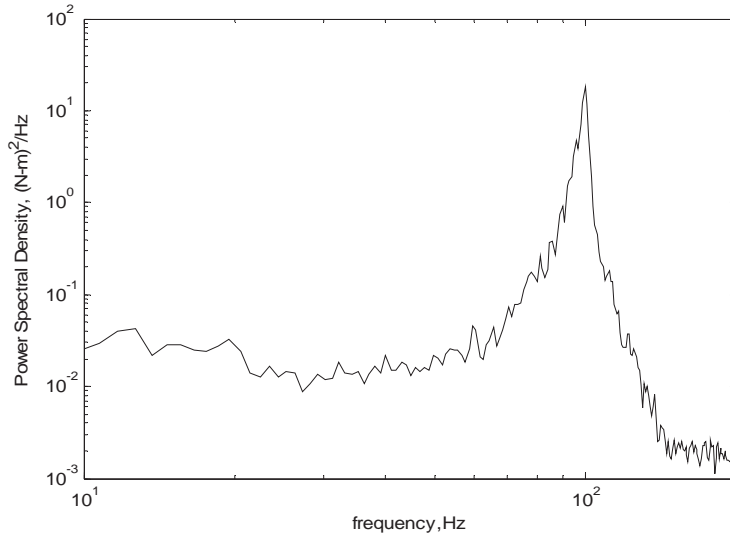


Fig. 6. Spectrum of the across wind base Bending moment ( $V = 28.65 \text{ m/s}$ ) – Chm4.

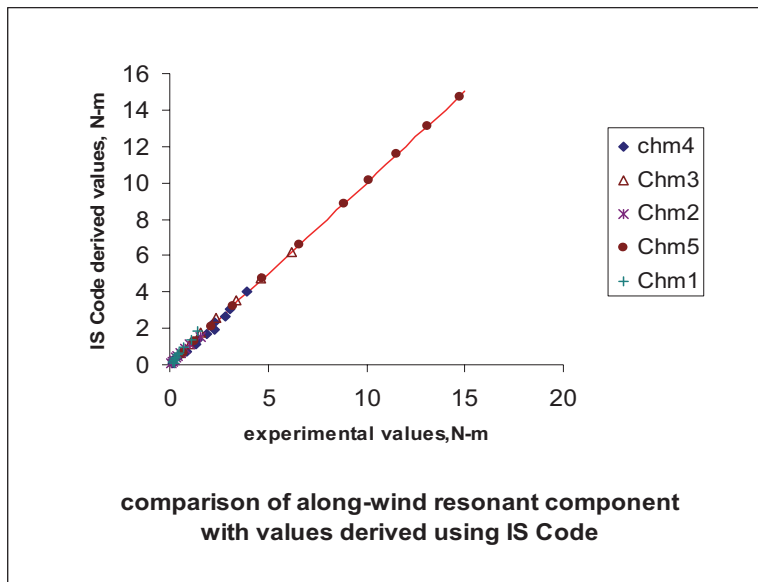


Fig. 7. Comparison of Resonant component of along-wind Response.

to chimneys which have significant taper. The fluctuating component of across wind response has been evaluated as the total variance of the combined vortex shedding and resonant frequency ranges in the region of  $0.5V_{cr}$  to  $2.0V_{cr}$ , where,  $V_{cr}$  is the critical velocity evaluated as  $(n_0 D/S)$  where  $n_0$  is the fundamental frequency of the chimney,  $D$  is the effective diameter at  $5/6$  times height of chimney and  $S$  is the Strouhal Number taken as 0.18 as seen from the experiments. The velocity scaling is 1.0 for all experiments. The tests conducted on models of isolated chimneys have shown that the design values obtained by extrapolation of wind tunnel results on along wind load effects have been in good agreement with IS Code recommendations at design wind speeds. The only corrections to be made are for the mean  $C_D$  and for observed damping ratios obtained in the models. The resonant components of along wind responses match very well with code recommendations at all

wind velocities as shown in Fig.7. It has always been a difficult exercise to evaluate the across wind responses with the same amount of confidence even around the critical wind speeds. Based on the trend of observations it is seen that beyond 1.5 times critical wind speed in chimneys with little taper near the top 1/3<sup>rd</sup> region, and 2 times the critical wind speed in case of chimneys with significant taper, only buffeting response is present in the across wind direction.

The values of ratio ( $R_1$ ) of rms across wind responses to the resonant component of rms along wind responses are shown in Fig.8(a) and Fig.8(b) for the deflection and bending moment respectively. In this figure  $R_1(Def)$  indicates the ratio corresponding to deflections and  $R_1(B.M)$  indicates the ratio corresponding to the Bending Moments. It is very clear that this ratio attains a maximum value at critical wind speed. Since most of the models had intensity of turbulence in the range of

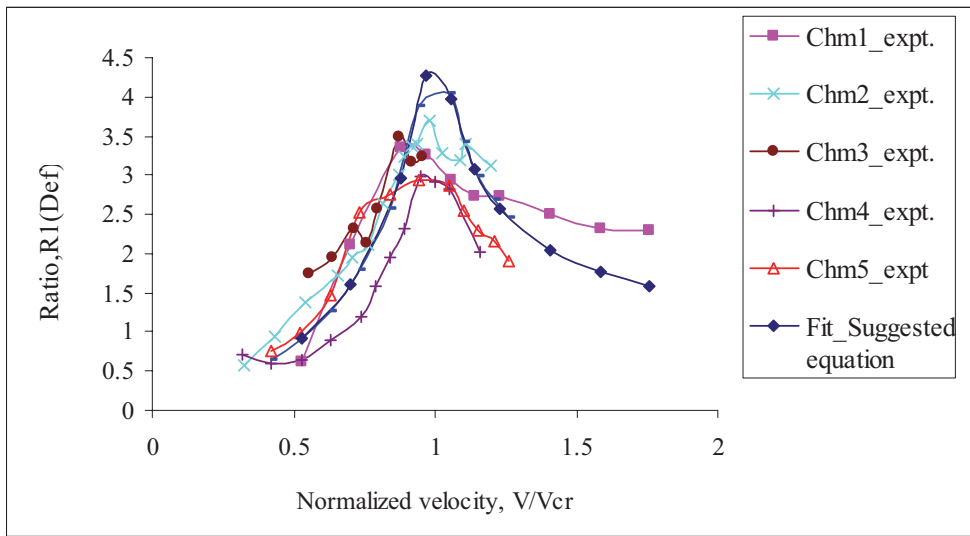


Fig. 8(a). Variation of  $R_1$  (Def) with normalized velocity.

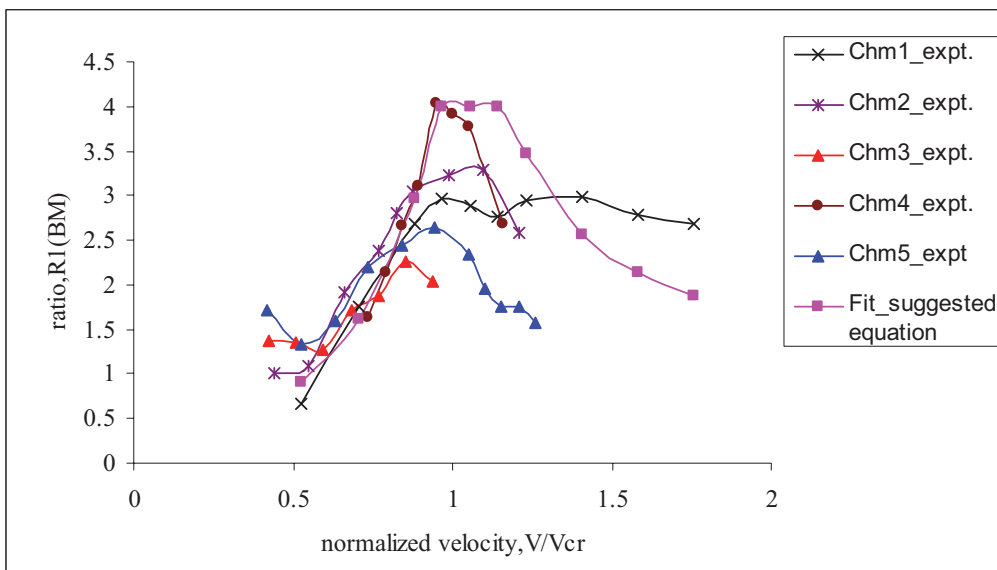


Fig. 8(b). Variation of  $R_1$  (B.M) with normalized Velocity.

7.5 to 10.0%, a uniform value of the same was considered as 0.10. Based on the above, a rough estimate for the ratio of across wind response to resonant along wind response was suggested as

$$R_1 = \frac{\left| \frac{V}{V_{cr}} \right|}{\left( \left| 1 - \frac{V}{V_{cr}} \right| \right) + 0.2 \left( \frac{V}{V_{cr}} \right)} \quad 0.6 < V/V_{cr} < 2.0 \quad (4)$$

The maximum value of  $R_1$  is limited to 5.0. The next stage of evaluation was to evaluate the resonant component of along wind response using IS: 4998 – 1992 provisions, for both bending moment and deflection. Using the model scale ratios, the corresponding responses were evaluated for all the chimney models. The responses were corrected for mean  $C_D$  as observed in tests to 0.8 as given in IS: 4998 for full-scale chimneys. The damping ratios obtained from free vibration traces on models were used in the computation. The across wind response at various wind speeds was evaluated using the parameter  $R_1$  as defined in equation no.4. Also the experimentally obtained along wind resonant responses were also used. The across wind responses obtained on two chimney models significantly deviated from the experimental response. This was investigated further using the available information.

The mean value of  $C_D$  can be taken as constant up to  $Re = 2 \times 10^5$ . However, the value of  $C'_L$  drops, significantly beyond  $Re$  of  $0.75 \times 10^5$  as per the plots of Schewe (1983). The observations of Cheng and Melbourne (1983) indicate that mean  $C_D$  can be approximated as a constant up to  $Re = 2 \times 10^5$  and for high turbulent intensities as present in atmospheric boundary layer. For intensities of turbulence of the order of 0.075 to 0.10, the fluctuating components of loading  $C'_D$  and  $C'_L$  can be expressed approximately as given below based on Fig.9 &10.

$$C'_D = 0.275 - 0.125 \times 10^{-5} * Re \quad Re < 10^5$$

$$C'_L = 0.250 - 0.125 \times 10^{-5} * Re \quad Re < 10^5$$

Thus the value of  $(C'_D/C'_L)$  varies in between 1.1 to 1.25. If wind tunnel experiments are conducted for  $Re \leq 10^5$ , the fluctuating components of along wind and across wind loadings would be

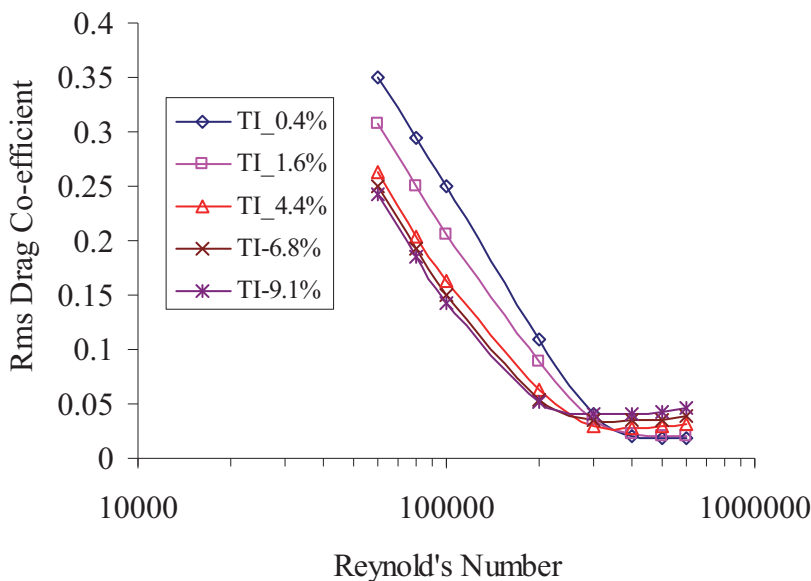


Fig. 9. Variation of fluctuating drag co-efficient with Reynolds Number (Cheung & Melbourne, 1983).



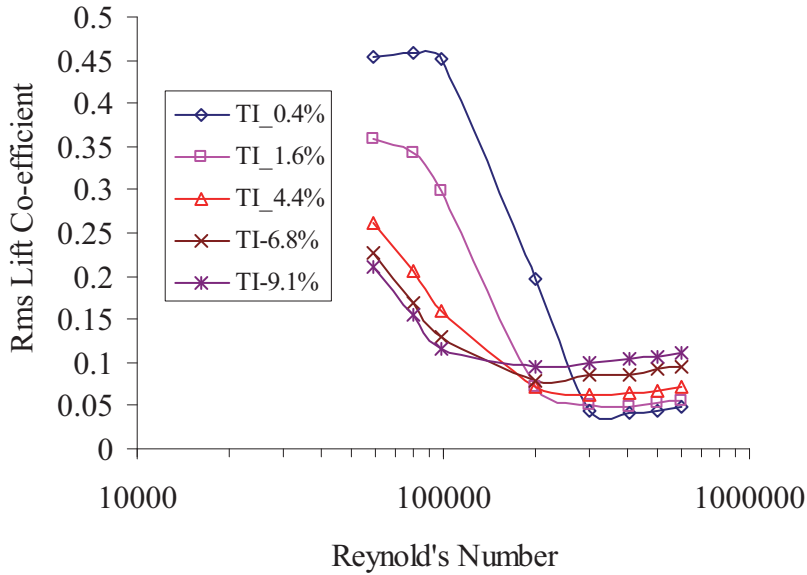


Fig. 10. Variation of fluctuating lift co-efficient with Reynold's Number (Cheung & Melbourne, 1983).

proportional. In the region of critical wind velocity, the response is dominated by the resonant component. There is significant increase in response in the velocity range where the front end of the bell shaped function of vortex shedding enters the resonant region, till the time the rear end of the bell shaped function leaves the resonant region. The maximum contribution to response is by resonant magnification. Hence, without loss of accuracy, the across wind response can be considered as proportional to along wind resonant component. The experiments indicate that a correction factor

$$C = \left( \frac{C'_L}{0.125} \right)$$

is to be used when  $Re > 10^5$  with  $C'_L$  being taken as

$$\begin{aligned} C'_L &= 0.25 - 0.125 * 10^{-5} * Re & 1 \times 10^5 < Re < 1.4 \times 10^5 \\ &= 0.075 & Re > 1.4 \times 10^5 \end{aligned}$$

Another important parameter could be the ratio of mean  $C_D$  to  $C'_L$  in full scale chimneys and models. Based on the IS: 4998(part-1)-1992 values of mean  $C_D$  to  $C'_L$

$$\left( \frac{C_D}{C'_L} \right)_{full-scale} = \frac{0.8}{0.125} \approx 6.0$$

If the tests are conducted such that the ratio of  $C_D$  to  $C'_L$  is around 6.0, the direct extrapolation of wind tunnel results to full-scale results is feasible. The value of mean  $C_D$  in wind tunnels is between 1 and 1.20. Thus if the tests are conducted in the range of  $Re$  between  $0.6 \times 10^5$  to  $1 \times 10^5$  at critical wind speed, then the results can be directly extrapolated to full-scale. Table: 2 shows the  $Re$  at critical wind speed and the range of  $Re$  in which the experiments are conducted:

Two of the models required correction and the corrected across wind response matched well with the experimental observations. The comparison of the typical across wind responses of rms deflection and bending moments are given in Fig. 11 to Fig. 12 for chimney models 4 and 5.

Table 2. Range of Reynolds number in wind tunnel tests.

S. No.	Reynold's Number x 10 <sup>5</sup>	
	Critical Wind Speed	Testing Range
1	0.365	0.19 – 0.64
2	0.6	0.20 – 0.73
3	1.72	0.57 – 1.72
4	1.06	0.33 – 1.22
5	1.44	0.64 – 1.92

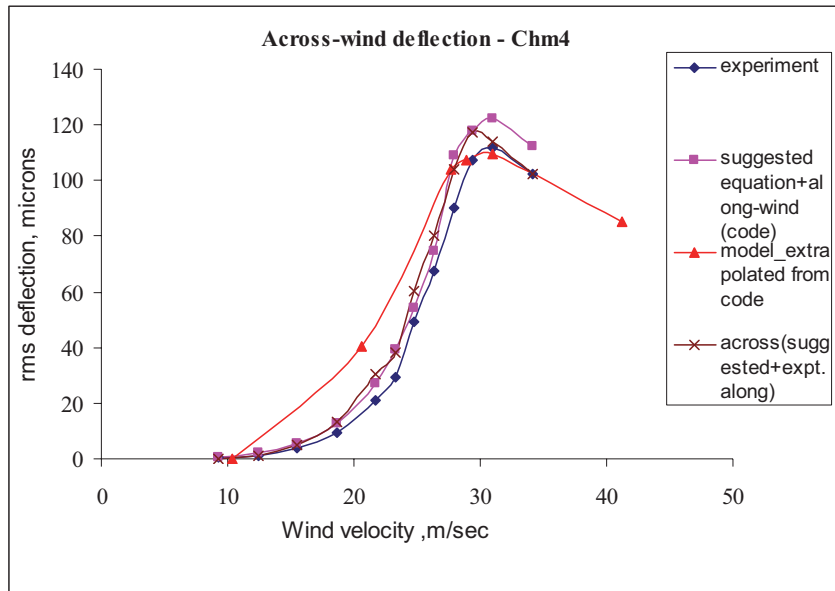


Fig. 11(a). Comparison of RMS across wind responses for Chm4.

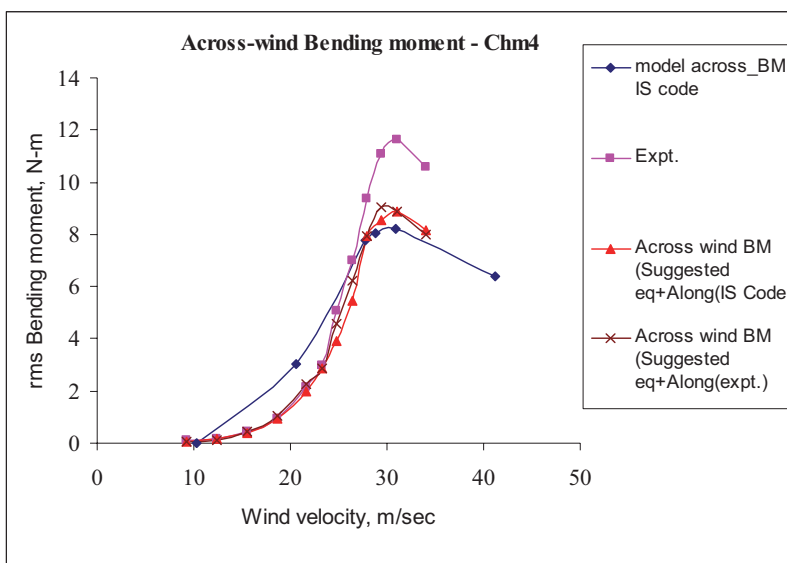


Fig. 11(b). Comparison of RMS across wind responses for Chm4.

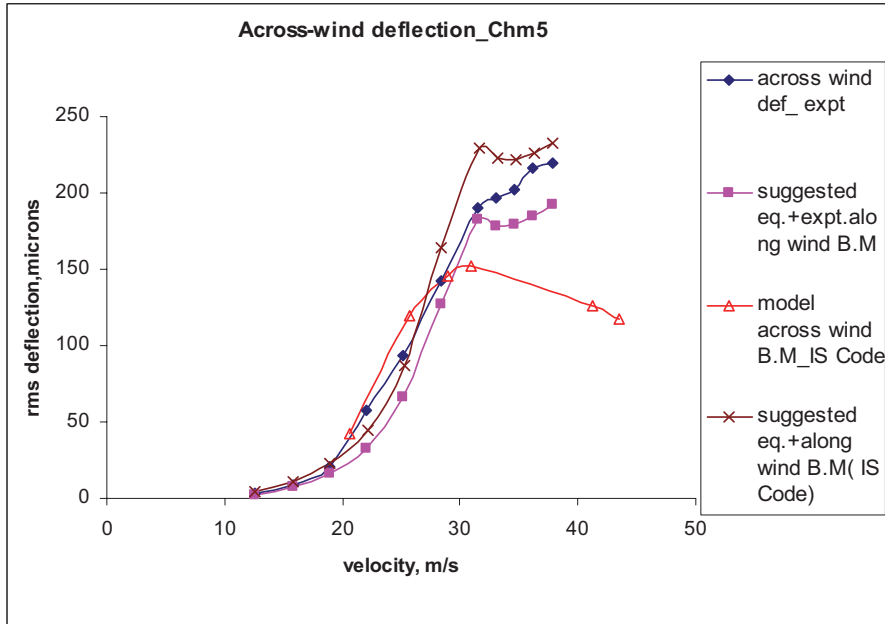


Fig. 12(a). Comparison of RMS across wind responses for Chm5.

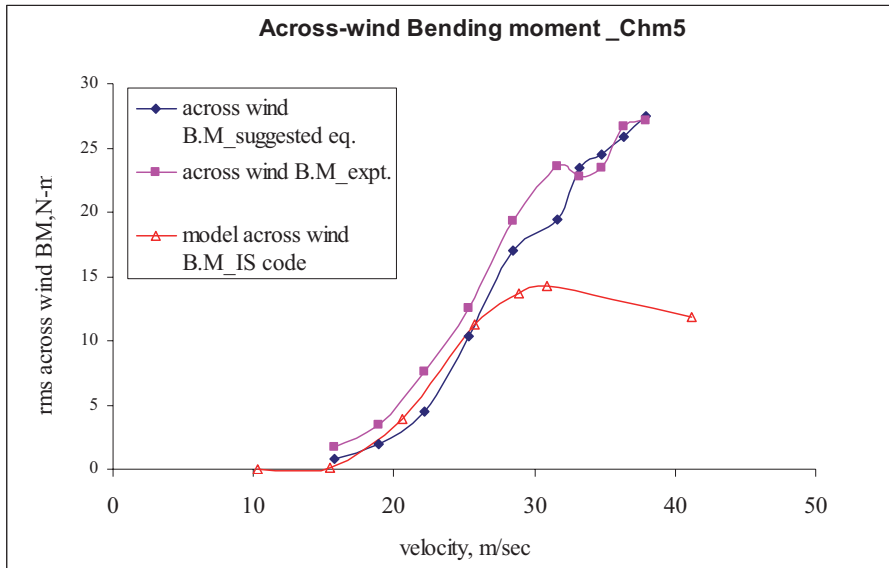


Fig. 12(b). Comparison of RMS across wind responses for Chm5.

### Full-scale Experiments (Literature)

The above procedure was adopted to predict the response of three full-scale chimneys, for which details are available in literature. The expression available in IS: 4998 were used to obtain the along wind resonant component. The across wind resonant component was derived using the suggested ratio based on  $(V/V_{cr})$  and intensity of turbulence up to  $1/3^{\text{rd}}$  height of chimney. The predicted behaviour matches reasonably well over the region  $0.6 (V/V_{cr})$  to  $1.5 (V/V_{cr})$ . It is

believed that beyond  $1.5 (V/V_{cr})$  in case of straight chimneys, and  $1.75 (V/V_{cr})$  in case of tapered chimneys the response would be essentially buffeting in nature. The responses obtained using the suggested procedure is given in Fig.13 and Fig.14. Tamura has given full scale experimental values of along-wind across-wind tip accelerations. These are reproduced in Fig.15. The ratio of across-wind response to along-wind response matches well with the ratio suggested in equation 4 as seen from Fig. 16.

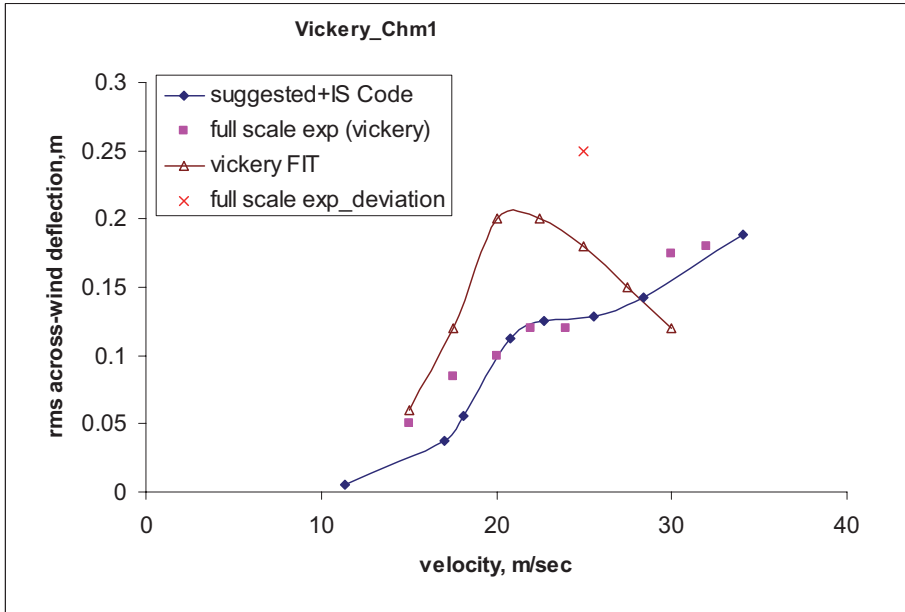


Fig. 13. Comparison with Full Scale Experimental Data (Vickery\_Chm1).

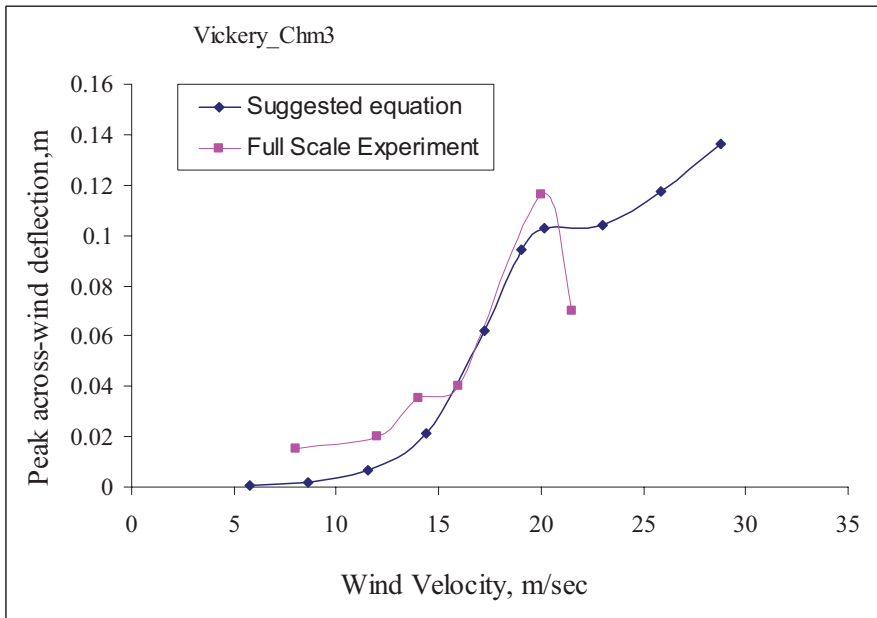


Fig. 14. Comparison with Full Scale Experimental Data (Vickery\_Chm3).

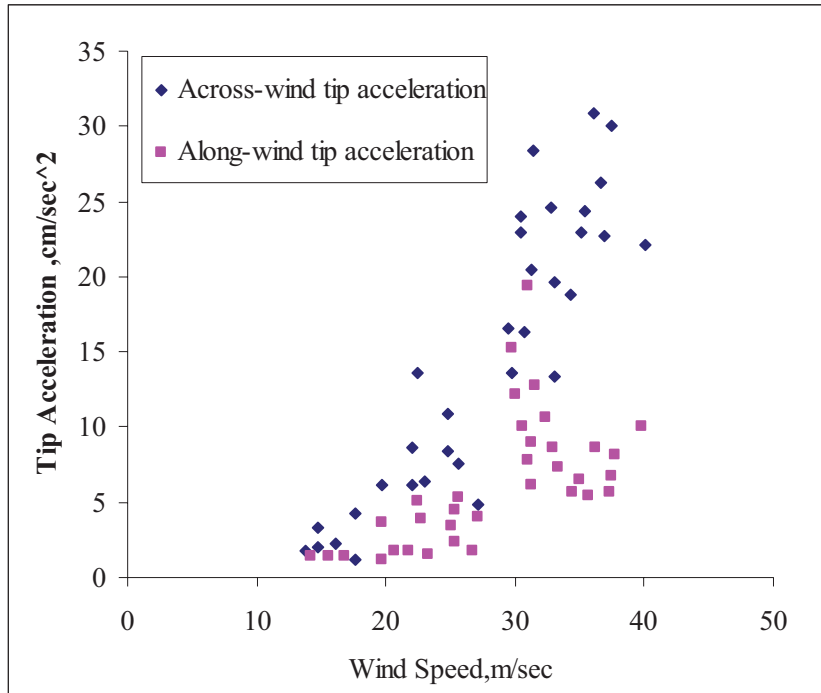


Fig. 15. Full Scale Experimental Data (Tamura\_1990)

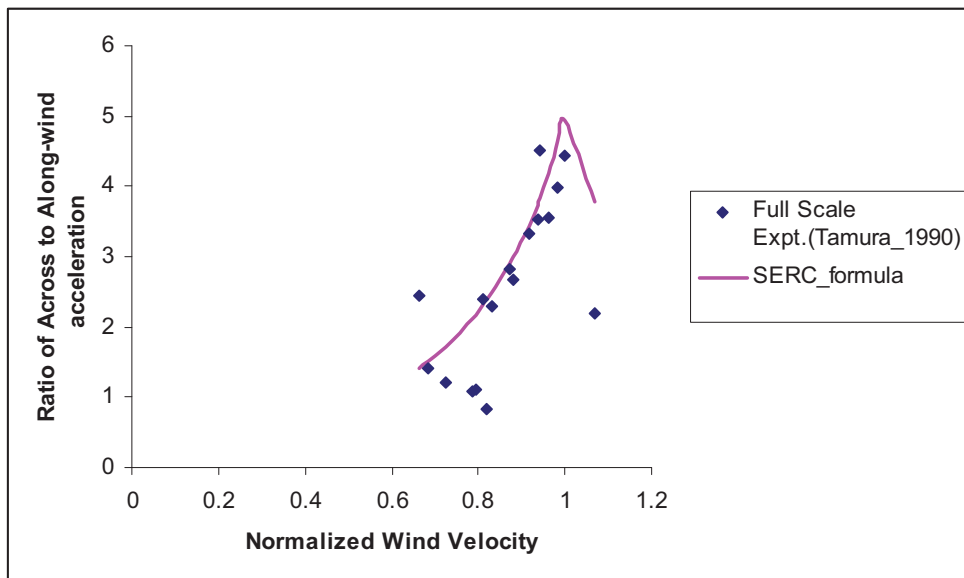


Fig. 16. Comparison with Full Scale Experimental Data

### Parametric Study

For conducting the parametric study the provisions of the across-wind response given in ACI: 307(2008) and the provisions of along-wind response given in IS: 4998(Part1)-1992 have been

used. The resonant component of along-wind response can be obtained as

$$\hat{M}_{al} = (g_f r) \bar{M} \sqrt{\frac{SE}{\beta}} \quad (5)$$

where  $\hat{M}_{al}$  = peak along-wind resonant base bending moment

$\bar{M}$  = Mean along-wind base bending moment at  $\bar{V} = V_{cr}$  at 5/6 height.

$g_f$  = statistical peak for longitudinal fluctuating component

$r$  = roughness parameter equivalent to twice the turbulence intensity

the values of  $g_f, r, S, E, \beta$  are calculated by using the expressions given in IS:4998.

The peak across-wind responses are given by

$$\hat{M}_{ac} = 5.0 (g_f r) \bar{M} \sqrt{\frac{SE}{\beta}} \quad (6)$$

where  $\hat{M}_{ac}$  = peak across-wind base bending moment

Similarly, the peak across wind deflection is given by

$$\hat{\delta}_{ac} = 5.0 (g_f r) \bar{\delta} \sqrt{\frac{SE}{\beta}} \quad (7)$$

where  $\bar{\delta}_{ac}$  = peak across-wind deflection

and  $\bar{\delta}$  = mean along-wind deflection

The variation of across-wind base bending moment with normalized wind speed is proposed as

$$\hat{M}_{ac,v} = \hat{M}_{ac} \cdot R_2 \quad (8)$$

Where

$$R_2 = 0.35 \left[ \frac{\left| \frac{V}{V_{cr}} \right|}{\left| 1 - \frac{V}{V_{cr}} \right| + 0.2 \frac{V}{V_{cr}}} \right] \quad (9)$$

$$\leq 1.0$$

The across-wind tip deflection based on ACI code was obtained using

$$\hat{\delta}_{ac} = \frac{\hat{M}_{ac}}{4\pi^2 f_0^2 \int_0^H m(z) \phi(z) z dz} \quad (10)$$

where  $m(z)$  is the mass per unit height of chimney at level  $z$  (kg/m)

$\phi(z)$  is the mode shape corresponding to first mode and

$f_0$  is the fundamental natural frequency of the structure, Hz

A total of 10 chimneys with different geometric properties were investigated for two values of modulus of elasticity viz.,  $3 \times 10^4$  and  $4 \times 10^4$  MPa. The geometric properties of the chimneys chosen for this parametric study are given in Table No.3. Table No. 5 gives the comparison of the

**Table 3.** Geometric Properties of the Chimneys chosen for the parametric study.

S.No	Chimney No.	Modulus of elasticity, N/m <sup>2</sup>	Height,m	Bottom diameter, m	Top diameter, m	Thickness at bottom, m	Thickness at top, m	Effective thickness,m
1,11	A1,B1	3E+10,4E+10	200	20	15	0.75	0.2	0.4475
2,12	A2,B2	3E+10,4E+10	225	22.5	15	0.75	0.25	0.475
3,13	A3,B3	3E+10,4E+10	250	25	15	0.9	0.35	0.5975
4,14	A4,B4	3E+10,4E+10	275	25	15	0.9	0.35	0.5975
5,15	A5,B5	3E+10,4E+10	300	27.5	17.5	1	0.35	0.6425
6,16	A6,B6	3E+10,4E+10	200	20	15	0.5	0.15	0.3845
7,17	A7,B7	3E+10,4E+10	225	22.5	15	0.65	0.2	0.5015
8,18	A8,B8	3E+10,4E+10	250	25	15	0.8	0.25	0.6185
9,19	A9,B9	3E+10,4E+10	275	27.5	15	0.9	0.25	0.6855
10,20	A10,B10	3E+10,4E+10	300	35	17.5	1	0.25	0.7525

**Table 4.** Across-wind base bending moments and deflections - ACI code and the simplified method suggested.

S. No	Chm No.	V <sub>max</sub> (ACI), m/s	V <sub>max</sub> suggested, m/s	M <sub>ac1</sub> *10 <sup>-9</sup> , N-m	M <sub>ac2</sub> *10 <sup>-9</sup> , N-m	M <sub>ac1</sub> /M <sub>ac2</sub>	Resonant Along Defln, m	Across Defln, m	Deflne ratio
1	A1	40.5	37.5	0.52	0.524	0.992	0.041	0.18	4.46
2	A2	31.2	32.5	0.46	0.435	1.057	0.034	0.174	5.1
3	A3	27.2	28.3	0.41	0.38	1.079	0.023	0.148	6.34
4	A4	22.4	23.3	0.315	0.275	1.145	0.02	0.114	5.43
5	A5	24.6	25.7	0.54	0.488	1.107	0.03	0.173	5.72
6	A6	37.7	34.9	0.493	0.505	0.976	0.039	0.179	4.57
7	A7	30.3	31.5	0.484	0.474	1.021	0.027	0.143	5.34
8	A8	26.6	27.7	0.53	0.49	1.082	0.032	0.194	5.97
9	A9	29.7	27.5	0.53	0.49	1.082	0.026	0.136	5.27
10	A10	33.8	35.2	1.31	1.285	1.019	0.026	0.139	5.3
11	B1	41.4	43.1	0.685	0.699	0.98	0.041	0.24	5.9
12	B2	38.3	37.5	0.62	0.59	1.051	0.034	0.16	4.63
13	B3	31.2	32.5	0.54	0.506	1.067	0.023	0.146	6.28
14	B4	25.9	27	0.42	0.372	1.129	0.02	0.127	6.15
15	B5	28	29.2	0.7	0.635	1.102	0.027	0.145	5.32
16	B6	43.9	40.7	0.67	0.69	0.971	0.04	0.184	4.56
17	B7	34.8	36.3	0.64	0.635	1.008	0.027	0.142	5.29
18	B8	32.4	33.8	0.68	0.67	1.015	0.022	0.116	5.24
19	B9	30.3	31.5	0.7	0.67	1.045	0.025	0.134	5.27
20	B10	39.2	40.8	1.7	1.75	0.971	0.027	0.135	5.03

across-wind base bending moments and deflections obtained using the rigorous analysis given in the ACI code and the simplified method suggested as also the wind speeds where maximum across-wind response occurs. The mean value of deflection ratio is observed to be 5.36, which is pretty close to 5 suggested for base bending moment. The ratio of peak across-wind deflection to peak along-wind resonant deflection is also included in the table 5. The mean value is found to be 5.35.

The mean value of the ratio of  $M_{ac}$ (ACI) to  $M_{ac}$ (suggested) is 1.045 with a standard deviation of 0.054. The ACI code recommends that across-wind response be evaluated, when the critical wind speed lies in the region of mean wind velocity values between 0.5 to  $1.3V_{zcr}$ , where  $V_{zcr}$  corresponds to the mean design wind speed at 5/6<sup>th</sup> height of the chimney. The typical profiles of the across-wind base bending moment variations suggested compared with the ACI recommendations are given in Fig 17 to Fig 20, which match very well.

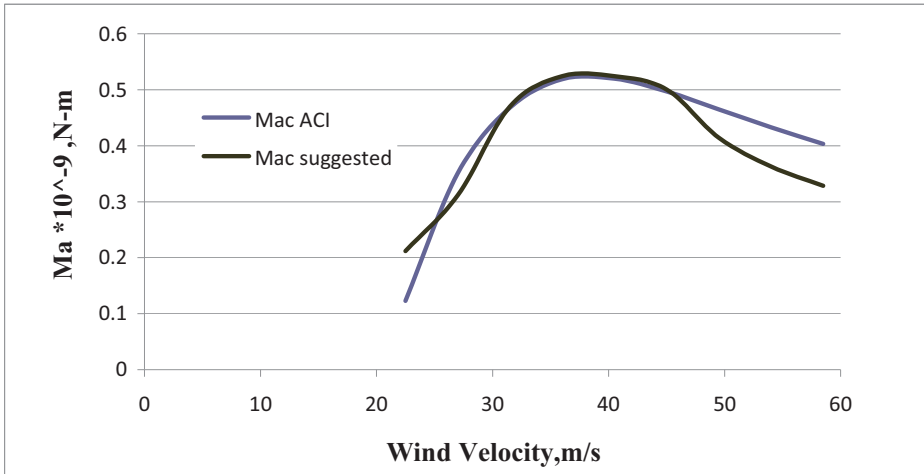


Fig. 17. Across wind Response of Chimney (Case A1).

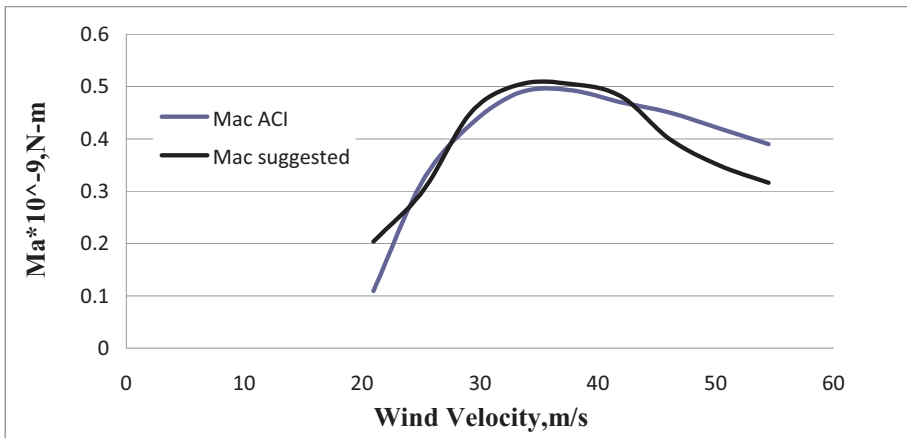


Fig. 18. Across wind Response of Chimney (Case A6).

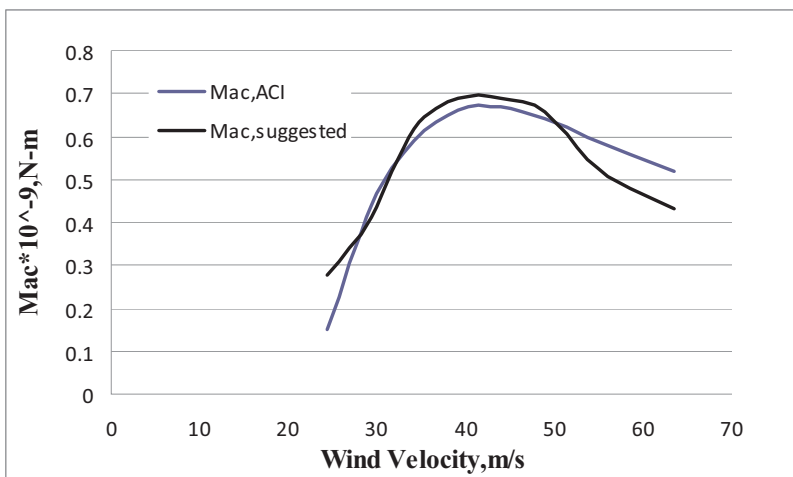


Fig. 19. Across wind Response of Chimney (Case B7).



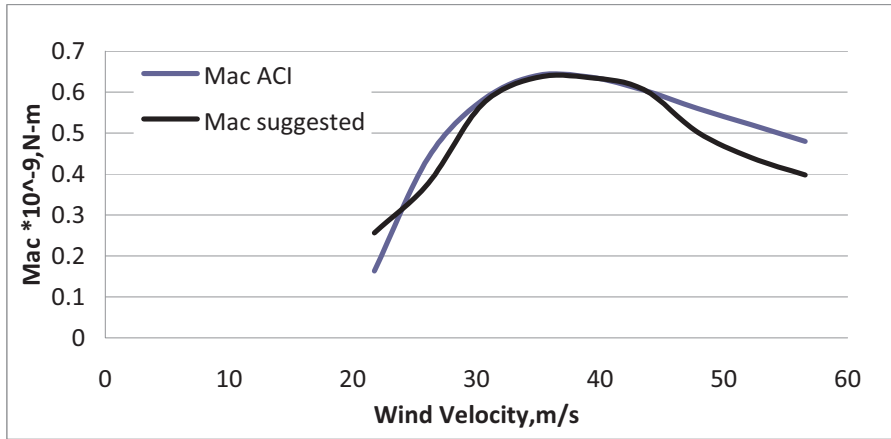


Fig. 20. Across wind Response of Chimney (Case B8).

## Conclusions

A brief review of literature enumerating the phenomenological model used in most codes of practice, including IS: 4998-1996 was carried out. Many investigators have felt that across-wind response of chimneys is not easily predictable based on wind tunnel experiments. A systematic investigation on five models of chimneys with scale ratio of 1:250 to 1:300 was carried out in the wind tunnel at varying wind speeds. In all the cases, the estimated value of  $V_{cr}$  was obtained using the relation  $V_{cr} = (n_o \cdot D/S)$  where ' $n_o$ ' is natural frequency, ' $D$ ' is the diameter at 5/6<sup>th</sup> height of chimney, and ' $S$ ' is the Strouhal's number taken as 0.18. The data was analyzed for rms component of along-wind response, and rms value of across-wind response in the region of  $0.6 \leq \frac{V}{V_{cr}} \leq 2.0$ . In this region, it is seen that the spectrum of vortex shedding interacts with the

resonant region leading to very high amplitudes. Since the phenomenon is closer to resonant region of across-wind response, a ratio of rms value of across-wind response to resonant component of along-wind response was considered. Based on the analysis of voluminous test data, the peak across-wind responses are given by

$$\hat{M}_{ac} = 5.0(g_{f,r})\bar{M}\sqrt{\frac{SE}{\beta}}$$

The variation of across-wind base bending moment with normalized wind speed is proposed as

$$\hat{M}_{ac,v} = \hat{M}_{ac} \cdot R$$

$$\text{Where } R = 0.35 \left[ \frac{\left| \frac{V}{V_{cr}} \right|}{\left| 1 - \frac{V}{V_{cr}} \right| + 0.2 \frac{V}{V_{cr}}} \right]$$

$$\leq 1.0$$

The above model predicts very well the full-scale and model responses of the chimneys studied in the present investigation.

## References

- Vickery, B.J., and Daly, A, "Wind Tunnel Modelling as a Means of Predicting the Response of Chimneys to Vortex shedding", *Engineering Structures*, vol.6, Oct 1984, pp. 363–368.
- Tamura, Y., and Nishimura, I., "Elastic Model of Reinforced Concrete Chimney for wind Tunnel Testing", *Journal of Wind Engineering and Industrial Aerodynamics*, vol. 33, 1990, pp. 231–236.
- Holmes, J.D., *Wind Loading of Structures*, Spon Press, 2001.
- Devdas Menon and Srinivasa Rao, P., "Uncertainties in Codal Recommendations for Across Wind Load Analysis of RC Chimneys", *Journal of Wind Engineering and Industrial Aerodynamics*, vol. 72, 1997, pp. 455–468.
- ACI: 307–08, *Code Recommendations for Design of Reinforced Concrete Chimneys*, pp. 307–01 to 307–30.
- Vickery, B.J., "The Response of Chimneys and Tower Like Structures to Wind Loading", *State the Art Volume in Wind Engineering*, International Association of Wind Engineering, 1995, pp. 205–233.
- Vickery, B.J., and Basu, R.I., " The Response of Reinforced concrete Chimneys to Vortex Shedding", *Journal of Engineering Structures*, vol. 6, 1984, pp. 324–333.
- Vickery, B.J., and Barn, R.I. " Across wind Vibration of Structures – Part I, Development of Mathematical Model for Two dimensional conditions", *Journal of Wind Engineering and Industrial Aerodynamics*, vol. 12(1), 1983, pp. 49–74.
- Flaga, A., and Liperki, T., "Code Approach to Vortex Shedding and Model", *Engineering Structures*, vol. 32, 2010, pp. 1530–1536.
- Cheung, J.K., and Melbourne, W.H., "Turbulence effects on some aerodynamic parameters of a circular cylinder at Super Critical Reynolds Numbers", *Journal of Wind Engineering and Industrial Aerodynamics*, Vol. 14, 1983, pp. 399–410.
- IS: 4998 – 1992, Part 1, *Criteria for Design of Reinforced Concrete Chimneys – Assessment of Loads*, Bureau of Indian Standards, New Delhi, 1992.